Protein Res. **36**, 544 (1990).
18. S. B. H. Kent *et al.*, in *Viral Proteinases as Therapeutic Targets*, E. Wimmer and H. G. Kräusslich, Eds. (Cold Spring Harbor Laboratory, Cold Spring Harbor, NY, 1989), pp. 223–230.
19. The HIV-1 PR analog containing a thioester bond replacement for the peptide bond at Gly^{51}-Gly^{52} was indefinitely stable (no detectable breakdown over several weeks) under the ligation reaction conditions at pH 4.3 (Fig. 3). However, model studies of the ligation reaction indicated that the thioester pseudopeptide bond was labile at higher pH. The ($[NHCH_2COSCH_2CO]^{51-52}Aba^{67,95}$)HIV-1 PR underwent hydrolysis forming HIV-1 PR(1-50,Gly-αCOOH) and $HSCH_2CO$(53-99)HIV-1 PR, with a half life of 2 hours at pH 7.5. Hydrolysis of thioesters is base catalyzed, and the rate of hydrolysis will be proportional to the concentration of hydroxide ion. The thioester analog of HIV-1 PR is thus quite stable over the pH range (pH 4 to 6) [A. D. Richards, R. Roberts, B. M. Dunn, M. C. Graves, J. Kay, *FEBS Lett.* **247**, 113 (1989)] and times (hours to days) normally used to study this enzyme. The HIV-1 PR is itself subject to autolytic digestion [J. E. Strickler *et al.*, *Proteins* **6**, 139 (1989)] and has a limited lifetime (hours to days) in solution. For this reason, we routinely store the native enzyme in 6 M GuHCl, conditions comparable to the ligation reaction conditions. Samples of enzyme stored in this way may be diluted directly into assay buffer for activity studies.
20. B. Koppenhoefer and V. Schurig, *Org. Synth.* **64**, 230 (1985).
21. H.-C. Cheng and D. Yamashiro, *Int. J. Peptide Protein Res.* **38**, 70 (1991).
22. R. Offord, *Protein Eng.* **4**, 709 (1991).
23. Amino acid sequences of the peptide segments. Amino-terminal half, HIV-1 PR(1-50, Gly-αCOSH): (H)-P^1QITLWQRPL^{10} VTIRIGGQLK^{20} EALLDTGADD^{30} TVLEEMNLPG^{40} KWKPKMIGGI^{50} G^{51} (αCOSH); carboxyl-terminal half, ($BrCH_2CO$(53-99)]HIV-1 PR: ($BrCH_2$-CO)-F^{53}IKVRQYD^{60} QIPVEI Aba^{67} GHK^{70} AIGTVLVGPT^{80} PVNIIGRNLL^{90} TQIG Aba^{95} $TLNF^{99}$-(OH). Aba is L-α-amino-*n*-butyric acid and substitutes for the two Cys residues 67 and 95 in HIV-1 PR (SF2 isolate) (*24*).
24. The native sequence of HIV-1 PR contains Cys residues at positions 67 and 95 in each subunit. Previous studies in our laboratory have shown that replacement of the four Cys residues in the homodimeric enzyme by the noncoded, isosteric amino acid Aba resulted in a fully active enzyme analog [S. B. H. Kent *et al.*, in *Peptides 1990, Proceedings of the 21st European Peptide Symposium*, E. Giralt and D. Andreu, Eds. (ESCOM, Leiden, 1991), pp. 169–171]. Comparison of the crystal structure of the Cys-containing enzyme obtained by recombinant techniques [R. Lapatto *et al.*, *Nature* **342**, 299 (1989)] with the original structural data (*5*) generated with chemically synthesized [J. Schneider and S. B. H. Kent, *Cell* **54**, 363 (1988)] [$Aba^{67,95,167,195}$]HIV-1 PR showed that the four Cys residues in the recombinant enzyme are unpaired and that the Cys side chains have the same conformations as the Aba side chains in the chemically synthesized enzyme. In the studies reported here, the target sequence was [$Aba^{67,95,167,195}$]HIV-1 PR, avoiding the presence of Cys residues in the segments undergoing ligation. However, use of the sulfur nucleophile chemistry described here for the chemical ligation of large unprotected peptide segments is not contraindicated by the presence of Cys residues in the target protein molecule. In model studies, we find that the -αCOSH group carried out rapid nucleophilic attack on a bromoacetyl group even at low pH conditions where the alkyl-SH side chain of a Cys residue did not react (M. Schnölzer and S. B. H. Kent, unpublished results). Thus, the ligation reaction described in this work can be carried out in the presence of unprotected Cys residues.
25. F. A. Robey and R. L. Fields, *Anal. Biochem.* **177**, 373 (1989).
26. The assay was carried out by adding an aliquot of the ligation reaction mixture to a solution of 50 μM fluorogenic substrate in 100 mM MES buffer, pH 6.5. The sequence of the substrate is 2-aminobenzoyl-Thr-Ile-Nle-Phe(*p*-NO_2)-Gln-Arg-amide (*17*). Nle is L-norleucine.
27. We thank A. Jones for assistance with the MS aspects of this work, G. Lu for technical assistance in peptide synthesis, M. Miller for 2.0 Å coordinates of the HIV-1 PR–MVT101 complex, and C. Delahunty for the preparation of 4-[α-(Boc-Gly-S)benzyl]-phenoxyacetic acid. Support of this work by the Markey Foundation is gratefully acknowledged. M.S. is supported by an AIDS Scholarship from the Bundesministerium für Forschung und Technologie, Germany.

7 January 1992; accepted 2 March 1992

Cloning and Characterization of Inducible Nitric Oxide Synthase from Mouse Macrophages

Qiao-wen Xie, Hearn J. Cho, Jimmy Calaycay, Richard A. Mumford, Kristine M. Swiderek, Terry D. Lee, Aihao Ding, Tiffany Troso, Carl Nathan*

Nitric oxide (NO) conveys a variety of messages between cells, including signals for vasorelaxation, neurotransmission, and cytotoxicity. In some endothelial cells and neurons, a constitutive NO synthase is activated transiently by agonists that elevate intracellular calcium concentrations and promote the binding of calmodulin. In contrast, in macrophages, NO synthase activity appears slowly after exposure of the cells to cytokines and bacterial products, is sustained, and functions independently of calcium and calmodulin. A monospecific antibody was used to clone complementary DNA that encoded two isoforms of NO synthase from immunologically activated mouse macrophages. Liquid chromatography–mass spectrometry was used to confirm most of the amino acid sequence. Macrophage NO synthase differs extensively from cerebellar NO synthase. The macrophage enzyme is immunologically induced at the transcriptional level and closely resembles the enzyme in cytokine-treated tumor cells and inflammatory neutrophils.

Nitric oxide (NO) is a short-lived, gaseous radical that is the smallest biosynthetically derived secretory product of mammalian cells. Through oxidation of thiols, hemes, Fe-S clusters, and other nonheme iron prosthetic groups, NO regulates enzymes, alters vascular tone, platelet function, inflammation, neurotransmission, and lymphocyte proliferation, and mediates some of the cytotoxic action of murine macrophages against tumor cells and microbes (*1*).

In endothelium and neurons, transient synthesis of small amounts of NO is rapidly triggered by agonists that elevate Ca^{2+}. Increased intracellular Ca^{2+} alters the conformation of calmodulin, which binds to nitric oxide synthase (NOS) to activate NO production (*2*, *3*). In contrast, macrophages, hepatocytes, smooth muscle cells, fibroblasts, mesangial cells, and some tumor cells begin to produce NO several hours after exposure to cytokines and microbial products. These cells then release large quantities of NO for many hours by a

Q.-w. Xie, H. J. Cho, A. Ding, T. Troso, C. Nathan, The Beatrice and Samuel A. Seaver Laboratory, Division of Hematology-Oncology, Department of Medicine, Cornell University Medical College, New York, NY 10021. J. Calaycay and R. A. Mumford, Department of Biochemical and Molecular Pathology, Merck Sharpe & Dohme Research Laboratories, Rahway, NJ 07065. K. M. Swiderek and T. D. Lee, Division of Immunology, Beckman Research Institute of the City of Hope, Duarte, CA 91010.

*To whom correspondence should be addressed.

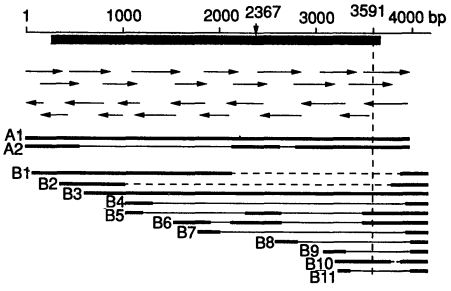

Fig. 1. Cloned iNOS cDNAs. cDNAs were cloned after immunoscreening with antibody to iNOS (*14*) and sequenced where indicated by the thick bars. Thin bars, regions not sequenced. Polyadenylated tails are not shown. The sequencing strategy was similar in each case and is illustrated for clone A1 by horizontal arrows. Clones A1, A2, and B1 included the ATG initiation codon within a consensus initiation sequence (GACATGG) (*15*). The dashed vertical line divides the nucleotide sequence into the region (base pairs 1 to 3591, numbered for clone A1) in which it was identical for all clones [except at position 2367 (vertical arrow)] and the remaining region (base pair 3592 to polyadenylate tails), where the A clones shared one sequence and the B clones shared an entirely different sequence. Black bar at top, longest coding region; horizontal dashes, deletions in the cDNA. GenBank accession number M87039.

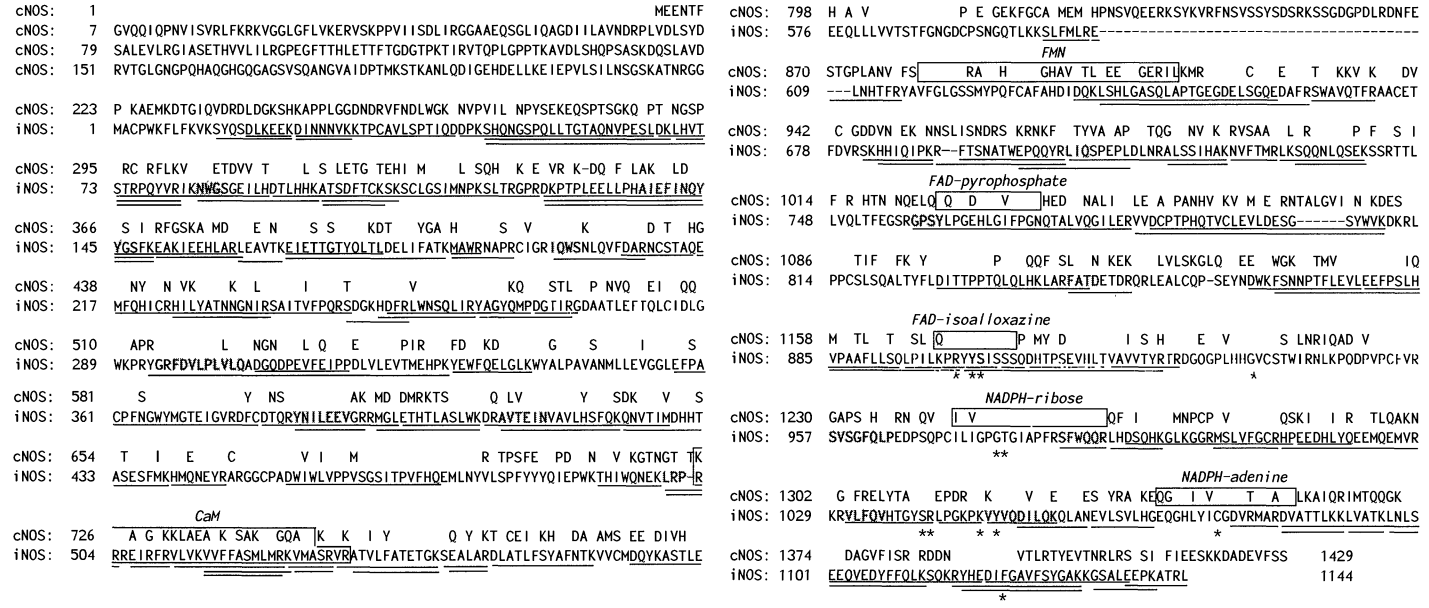

Fig. 2. Amino acid sequence (*16*) of iNOS and comparison to cNOS (*9*). For iNOS, shaded residues, 18 tryptic peptides that matched the deduced amino acid sequence, were sequenced by Edman degradation; underlined peptides were confirmed by LC-MS. Starred residues are predicted to represent nucleotide contact sites, based on modeling of the tertiary structure (*7*). Boxed residues are proposed to represent the nucleotide and calmodulin binding sites (CaM) of cNOS, based on analysis of primary sequence (*5*). Where cNOS residues are omitted, they match iNOS.

process that requires neither Ca^{2+} nor calmodulin (*1*, *4*). Although a deduced amino acid sequence for rat cerebellar NOS has been reported (*5*), constitutively expressed cerebellar NOS [termed cNOS (Ca^{2+}- and calmodulin-dependent)] may be the product of a different gene than immunologically inducible NOS [termed iNOS (Ca^{2+}- and calmodulin-independent). To investigate this, we cloned iNOS cDNA from activated mouse macrophages and confirmed most of the deduced amino acid sequence by mass spectrometry.

A polyclonal, monospecific rabbit antibody to iNOS purified from RAW 264.7 macrophagelike cells (American Type Culture Collection TIB 71) (*4*) identified 13 clones among 5×10^4 phages in a cDNA library prepared from RAW 264.7 cells activated with interferon-γ (IFN-γ) and lipopolysaccharide (LPS) (Fig. 1). The cDNA inserts in these clones contained overlapping portions of coding regions corresponding to two isoforms of the enzyme, A and B (Fig. 1). The A clones encoded a protein 22 amino acids shorter at the COOH-terminus, with ten terminal amino acids that differed from those in the B clones. The isoforms also differed at nucleotide 2367, where AGT encoded Ser^{704} in the A clones and AGG encoded Arg^{704} in the B clones. Finally, the mutually identical 3′ untranslated regions of the A clones differed completely from the mutually similar 3′ untranslated regions of the B clones. The amino acid sequence encoded by the B clones was confirmed in the pure protein for both of the distinguishing features in the coding region (see below). In contrast, at the protein level, no evidence was found for expression of the A isoform in RAW 264.7 cells. The deduced amino acid sequence of the longer (B) isoform contained 1,144 amino acids with a predicted molecular size of 130,556 daltons (Fig. 2).

To confirm the deduced amino acid sequence, we subjected purified, enzymatically active iNOS to tryptic digestion and Edman analysis. Eighteen tryptic peptides matched the deduced amino acid sequence (Fig. 2), which showed that the cDNA encoded iNOS but confirmed only 9% of the predicted amino acid sequence. More extensive confirmation of the amino acid sequence was obtained by liquid chroma-

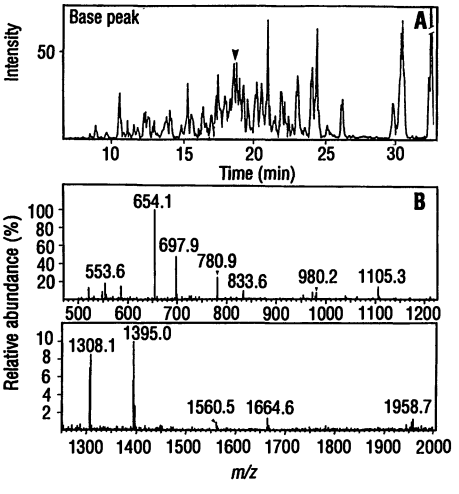

Fig. 3. Analysis by LC-MS. A tryptic digest of iNOS was separated on a C_{18} reversed-phase packed capillary column (0.25 mm interior diameter) at a flow rate of 2 μl/min with 0.1% aqueous trifluoroacetic acid and a gradient of 2 to 80% acetonitrile over 40 min. The effluent was fed directly to the electrospray interface of a Finnigan MAT TSQ-700 quadrupole mass spectrometer (*17*). The MacProMass program (*18*) was used to calculate values for all expected tryptic peptides, including those that resulted from incomplete digestion. Mass chromatograms spanning the *m/z* (mass-to-charge ratio) range 500 to 2000 were generated for each expected mass. For peptides larger than 1000 daltons, two or more charge states had to be present in the spectrum before an assignment was made. For peptides between 500 and 1000 daltons, assignments were based on a single ion, provided it could not be included in a series corresponding to a larger peptide. (**A**) Base peak chromatogram obtained by plotting the intensity of the most intense ion in a spectrum versus the elution time. Seven hundred forty-three scans (3-s cycle time) were collected. Arrowhead indicates the peak detailed in (B). (**B**) Mass spectrum for the average of scans 371 to 377. The ions correspond to both the +2 and +1 charge states of six different peptides. (The pairs are 553.6 and 1105.3, 654.1 and 1308.1, 697.9 and 1395.0, 780.9 and 1560.5, 833.6 and 1664.6, and 980.2 and 1958.7.) Four of these can be uniquely assigned to predicted products of the tryptic digest of iNOS: 1308.1 is (R)VLFQVHTGYSR(L) (residues 1031 to 1041); 1395.0 is (R)VRATVLFATETGK(S) (residues 531 to 543); 1664.6 is (K)SLFMLRELNHTFR(Y) (residues 602 to 614); and 1958.7 is (R)DFCDTQRYNILEEVGR(R) (residues 376 to 391) (*16*). The peptide of 1105 daltons has two possible assignments, either (K)VYVQDILQK(Q) (residues 1048 to 1056) or (R)MARDVATTLK(K) (residues 1081 to 1090) (*16*), although the peptide of 1560 daltons did not correspond to a predicted tryptic fragment.

tography–mass spectrometry (LC-MS) (Fig. 3). Ions were identified as arising from tryptic peptides that comprised 65% of the deduced amino acid sequence of iNOS (Fig. 2). Analysis of the two proteolytic digests required a total of 30 pmol of iNOS and 1.5 hours of instrument time. For these studies, enzymatic digestion of iNOS was performed without prior reduction and alkylation. Cysteine residues were present in 12 of the 17 regions for which LC-MS did not provide sequence confirmation; these peptides may have been linked together.

The amino acid sequence of mouse macrophage iNOS is only 51% identical to the deduced sequence of rat cerebellar cNOS (Fig. 2) (5). Although both enzymes have 24 cysteines, only 16 are positionally conserved. The iNOS is shorter at the NH_2-terminus (222 residues), midportion (52 residues in five sites), and COOH-terminus (12 residues); these amino acids are presumably not necessary for catalysis. As for cNOS (5), the COOH-terminal half of iNOS is homologous to cytochrome P450 reductase (29% identical), the only other mammalian enzyme known to have both flavin mononucleotide (FMN) and flavin-adenine dinucleotide (FAD) as cofactors (6). By modeling analysis, the COOH-termini of iNOS and cNOS are likely to share regions of multistranded β sheet and surrounding α helices that are similar to portions of the nucleotide binding domains of crystallographically resolved ferredoxin–nicotinamide adenine dinucleotide phosphate ($NADP^+$) reductase (7). Discontinuous residues common to iNOS and cNOS are predicted to comprise the nucleotide contact sites (Fig. 2). These sites differ extensively from the cofactor binding sites designated by Bredt and coworkers on the basis of primary sequence homologies (Fig. 2) (5).

Because enzymatic activity of iNOS is independent of added calmodulin (4, 8), it was unexpected that amino acids 503 to 532 of iNOS consisted almost exclusively of basic and hydrophobic residues characteristic of calmodulin binding sites (9). In contrast to the high homology between iNOS and cNOS in other presumed cofactor binding sites, this region of iNOS was only 43% identical to the 21 residues designated as the presumptive calmodulin binding site of cNOS (Fig. 2) (5).

Enzyme activity of NOS (10) and chromatographically recognizable iNOS protein (4) have been observed in macrophages only after immunologic activation. We hypothesized that immunologic activation induces iNOS at the transcriptional level. This hypothesis was confirmed by the finding that RAW 264.7 cells expressed NOS enzyme activity, synthesized and accumulated iNOS mRNA (approximately 4.4 kb), and displayed iNOS antigen only after exposure to IFN-γ and LPS, and that actinomycin D inhibited each of these processes (Fig. 4). Likewise, a protein antigenically related to and having the same molecular size as iNOS from RAW 264.7 cells was detected by protein immunoblot in primary mouse peritoneal macrophages and EMT-6 mouse mammary adenocarcinoma cells (11) only after exposure to IFN-γ and LPS, as well as in rat neutrophils from an inflammatory exudate (Fig. 4B). Finally, in primary macrophages elicited by intraperitoneal injection of thioglycollate broth, iNOS was weakly stained by immunofluorescence in half the cells after exposure to IFN-γ alone or LPS alone, while approximately 85% of the cells expressed large amounts of iNOS antigen after treatment with IFN-γ and LPS in combination (Fig. 5).

We have combined cDNA sequencing and mass spectroscopy to establish most of the amino acid sequence of a large protein for which sequence information was not previously available. Analysis by LC-MS of overlapping tryptic and aspartate-N maps allowed us both to confirm and to order peptides comprising 78% of the sequence of iNOS. Confirmation of this much sequence by Edman degradation would require at least ten times more protein and over 1000-fold more instrument time, not counting the time to purify each peptide.

A protein closely related to macrophage iNOS appears to be widely distributed in

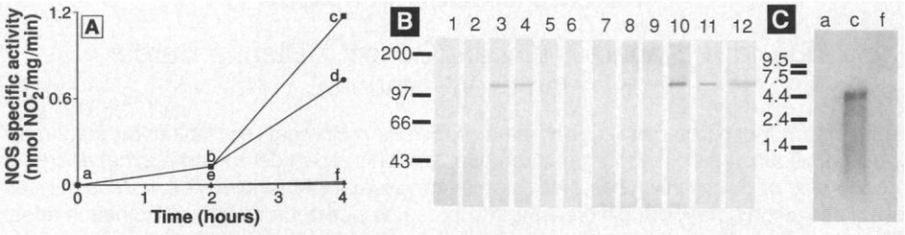

Fig. 4. Transcriptional induction of iNOS. (**A**) NOS enzyme activity in lysates of activated RAW 264.7 cells was measured as described (*4*). Recombinant mouse IFN-γ (10 ng/ml) and LPS (1 μg/ml) were added at time 0 (a). Samples were taken then, at 2 hours (b), and at 4 hours (c). Other cultures were treated with actinomycin D (0.2 μg/ml) at 2 hours and sampled 2 hours later (d), or treated with actinomycin D at time 0 and sampled at both 2 hours (e) and 4 hours (f). At each time, cell viability by Trypan blue exclusion exceeded 90%. ■, No actinomycin D; ●, actinomycin D at 2 hours; ▲, actinomycin D at 0 hours. (**B**) Protein immunoblot of iNOS induction. Lanes 1 through 6 correspond to cells from (A) in the order (a) through (f). Lanes 7 through 10 illustrate inducibility of iNOS in primary mouse peritoneal macrophages: lane 7, untreated; lane 8, treated with IFN-γ alone; lane 9, treated with LPS alone; and lane 10, treated with IFN-γ plus LPS. Lane 11 represents IFN-γ– and LPS-treated EMT-6 mammary adenocarcinoma cells (untreated cells or cells treated with IFN-γ alone were nonreactive). Lane 12 corresponds to rat peritoneal neutrophils elicited with oyster glycogen. Aliquots of the lysates (10 μg of protein, except 100 μg for neutrophils) were electrophoresed in a 7.5% polyacrylamide gel with SDS, electroblotted to nitrocellulose, probed with a 1:1000 dilution of IgG antibody to iNOS, and detected with a 1:1000 dilution of alkaline phosphatase–conjugated sheep antibody to rabbit IgG (Boehringer Mannheim). (**C**) Northern (mRNA) blot of RAW 264.7 cells treated as in (A); lanes are lettered to correspond. After electrophoresis in a 1% agarose gel with formaldehyde and transfer to a nylon membrane, the mRNA was hybridized with ^{32}P-labeled antisense RNA prepared from iNOS clone B3 (Fig. 1), which corresponded to amino acids 35 to 1144 and the 3′ untranslated region. (**D**) Nuclear run-on. Nuclei of RAW 264.7 cells treated and lettered as in (A) were used to synthesize ^{32}P-labeled RNA, which was hybridized to a filter blotted with the control plasmid pUC19 or piNOS, a pBluescript plasmid (Stratagene) that had an insert of iNOS cDNA clone B3.

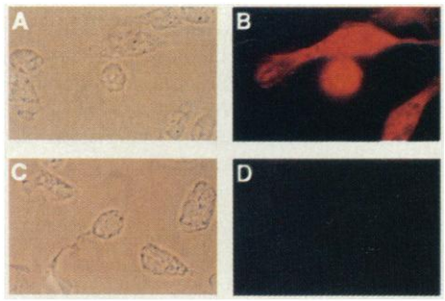

Fig. 5. Immunologic induction of iNOS in individual primary macrophages. Peritoneal macrophages were isolated from CD-1 mice (Charles River, Wilmington, Massachusetts) 4 days after an intraperitoneal injection of thioglycollate broth and incubated for 16 hours with IFN-γ (10 ng/ml) and LPS (1 μg/ml) (**A** and **B**) or without these agents (**C** and **D**). The cells were stained with antiserum to iNOS (1:1000) (*14*), and the bound antibody was detected with a 1:200 dilution of rhodamine-conjugated goat antibody to rabbit IgG and IgM (Jackson ImmunoResearch). (A) and (C) are phase-contrast views in bright-field; (B) and (D) are fluorescence views of the same field (×1000 magnification). There was no staining with preimmune serum. Results were similar with RAW 264.7 cells and EMT-6 mammary adenocarcinoma cells.

other activated or inflammatory cell populations. Nevertheless, our data establish that iNOS is distinct from cNOS. The two enzymes shared only 51% of their amino acid sequence and polyclonal antibody to iNOS did not react with recombinant rat cerebellar cNOS (*12*). Amino acid identity between iNOS and cNOS was high in regions provisionally identified as important for the binding of FAD and the reduced form of $NADP^+$ (NADPH), cofactors for which the two enzymes have similar requirements, but considerably less in the region presumed to bind calmodulin, for which the requirements of the enzymes differ dramatically.

Members of the NOS family appear to be better distinguished by their mode of activation than by the organ or cell type of their origin. Every organ is a mixture of cell types that includes endothelium (prototypic host cells for cNOS) and macrophages (prototypic host cells for iNOS) (*1*) and thus is likely to contain both enzymes under some circumstances. Even the same cell population may contain both a constitutive, agonist-activated, rapidly responsive, low-output NOS activity and a slowly induced, immunologically elicited, high-output NOS activity, perhaps reflecting the presence of both cNOS and iNOS within a single cell (*13*). Although cNOS is activated by elevation of intracellular Ca^{2+}, the major mechanism for activation of iNOS appears to be transcriptional induction.

REFERENCES AND NOTES

1. S. Moncada, R. M. J. Palmer, E. A. Higgs, *Pharmacol. Rev.* **43**, 109 (1991); L. J. Ignarro, *Biochem. Pharmacol.* **41**, 485 (1991); J. B. Hibbs, Jr., *et al.*, *Nitric Oxide from L-Arginine: A Bioregulatory System*, S. Moncada and E. A. Higgs, Eds. (Elsevier, Amsterdam, 1990), pp. 189–223; C. Nathan and J. B. Hibbs, Jr., *Curr. Opin. Immunol.* **3**, 65 (1991); D. J. Stuehr and O. W. Griffith, *Adv. Enzymol. Relat. Areas Mol. Biol.*, in press; Q.-w. Xie and C. Nathan, in *Cellular and Molecular Mechanisms of Inflammation*, C. Cochrane and M. Gimbrone, Eds. (Academic Press, New York, in press).
2. D. S. Bredt and S. H. Snyder, *Proc. Natl. Acad. Sci. U.S.A.* **87**, 682 (1990).
3. R. Busse and A. Mülsch, *FEBS Lett.* **265**, 133 (1990).
4. D. J. Stuehr, H. J. Cho, N. S. Kwon, M. F. Weise, C. F. Nathan, *Proc. Natl. Acad. Sci. U.S.A.* **88**, 7773 (1991).
5. D. S. Bredt *et al.*, *Nature* **351**, 714 (1991).
6. T. D. Porter, *Trends Biochem. Sci.* **16**, 154 (1991).
7. P. A. Karplus, M. J. Daniels, J. R. Herriott, *Science* **251**, 60 (1991); K. O. Elliston and M. W. Baum, unpublished observations; T. D. Lee *et al.*, in preparation.
8. Y. Yui *et al.*, *J. Biol. Chem.* **266**, 12544 (1991).
9. K. T. O'Neil and W. F. DeGrado, *Trends Biochem. Sci.* **15**, 59 (1990).
10. D. J. Stuehr *et al.*, *Biochem. Biophys. Res. Commun.* **161**, 420 (1989).
11. I. J. Amber, J. B. Hibbs, Jr., R. R. Taintor, Z. Vavrin, *J. Leukocyte Biol.* **44**, 58 (1988).
12. Q.-w. Xie *et al.*, unpublished observations.
13. S. Lamas, T. Michel, B. M. Brenner, P. A. Marsden, *Am. J. Physiol.* **261**, C634 (1991).
14. The RAW 264.7 murine macrophage cell line was activated with recombinant IFN-γ (rIFN-γ) (100 U/ml; Genentech, San Francisco, CA) and LPS (2 μg/ml) for 4 hours. Polyadenylated RNA with oligo(dT) as a primer was used to prepare a cDNA library in the Uni ZAP-XR unidirectional vector (Stratagene). Antiserum was raised by injecting a rabbit with 90 μg of 130-kD iNOS that was purified as described (*4*) from two 100-liter cultures of activated RAW 264.7 cells and emulsified with Freund's complete adjuvant, followed by two booster injections of incomplete Freund's adjuvant that contained 45 to 50 μg each of iNOS that was purified as above and additionally by isolation of the 130-kD region on SDS–polyacrylamide gel electrophoresis. Immunoglobulin G (IgG) antibody to iNOS was purified on immobilized recombinant protein G (Pierce), adsorbed with *Escherichia coli*, and used to screen the cDNA library.
15. M. Kozak, *J. Biol. Chem.* **266**, 19867 (1991).
16. Abbreviations for the amino acid residues are: A, Ala; C, Cys; D, Asp; E, Glu; F, Phe; G, Gly; H, His; I, Ile; K, Lys; L, Leu; M, Met; N, Asn; P, Pro; Q, Gln; R, Arg; S, Ser; T, Thr; V, Val; W, Trp; and Y, Tyr.
17. S. A. McLuckey, G. J. van Berkel, G. L. Glish, E. C. Huang, J. D. Henion, *Anal. Chem.* **63**, 375 (1991).
18. T. D. Lee and S. Vemuri, *Biomed. Environ. Mass Spectrom.* **19**, 639 (1990).

19. We thank P. Davies, A. Williamson, and J. Schmidt for advice; M. A. Palladino, Jr., and Genentech for rIFN-γ; K. Elliston and M. Baum for homology analysis; J. Aunins, C. Seamans, L. Egger, K. Glazomitsky, S. Grant, M. Silberklang, and M. Weise for their contributions to the scaled-up purification of iNOS; D. Stuehr for lysate of cNOS-transfected cells; J. B. Hibbs, Jr., for EMT-6 cells; S. Grant for rat peritoneal neutrophils; and J. MacMicking for review of the manuscript. Supported in part by NIH grants CA43610 and AI30165.

23 December 1991; accepted 25 February 1992

Chromosome Size-Dependent Control of Meiotic Recombination

David B. Kaback,* Vincent Guacci,† Dianna Barber, James W. Mahon

Smaller chromosomes have higher rates of meiotic reciprocal recombination (centimorgans per kilobase pair) than larger chromosomes. This report demonstrates that decreasing the size of *Saccharomyces cerevisiae* chromosomal DNA molecules increases rates of meiotic recombination and increasing chromosome size decreases recombination rates. These results indicate that chromosome size directly affects meiotic reciprocal recombination.

During meiosis I, homologous chromosomes pair, undergo reciprocal recombination (crossing-over), and then segregate from each other to reduce the number of chromosomes by half. Crossing-over is believed to be required to ensure proper pairing and segregation. Accordingly, in most organisms there is at least one crossover event between each pair of homologous chromosomes (*1*).

The total length of a chromosome's genetic map is a function of the total amount of meiotic reciprocal recombination on that chromosome. Genetic map lengths determined for most of the 16 chromosomes from the yeast *Saccharomyces cerevisiae* are close to complete and vary from 150 to 450 centimorgans (cM), indicating an average of three crossovers per meiosis for the smallest chromosome [250 kilobases (kb)] to nine crossovers for the largest [1650 kb, exclusive of the chromosome that contains ribosomal DNA (rDNA) because rDNA does not undergo meiotic recombination (*2, 3*)] (*4, 5*). From these results, it was concluded that DNA sequences on the smallest yeast chromosome must undergo recombination at a twofold higher average rate (0.6 cM/kb) than DNA sequences on the largest (0.3 cM/kb) (*4, 5*).

The mechanism enabling small *S. cerevisiae* chromosomes to undergo meiotic recombination at high rates is not understood. Various chromosomal sequences have been shown to undergo meiotic recombination at different rates, suggesting specific sequences may be involved in controlling recombination (*5–8*). However, the smallest yeast chromosome has a high recombination rate over most of its physical length (*5*), suggesting that chromosome size also may play a role.

To investigate the role of chromosome size in regulating meiotic recombination, we used strains in which the 250-kb chromosome *I* DNA molecule was bisected into functional half-chromosomes (*9*) (Fig. 1). Chromosome *I* was bisected at *CEN1*, producing chromosomes *IL* and *IR* that were 150 and 100 kb, respectively. Chromosome *I* also was bisected near the *MAK16* gene, giving chromosomes *IA* and *IB* that were 125 and 135 kb, respectively. Genetic markers were crossed onto each set of bisected chromosomes to enable measurement of recombination over large regions (Fig. 1A). Pulse-field gel electrophoresis (PFGE) confirmed that the marked strains contained

Department of Microbiology and Molecular Genetics, Graduate School of Biomedical Sciences, University of Medicine and Dentistry of New Jersey–New Jersey Medical School, 185 South Orange Avenue, Newark, NJ 07103.

*To whom correspondence should be addressed.
†Present address: Department of Embryology, Carnegie Institution of Washington, Baltimore, MD 21210.